

# Structural Optimization of a Joined Wing Using Equivalent Static Loads

H. A. Lee,\* Y. I. Kim,\* and G. J. Park†

Hanyang University, Ansan 425-791, Republic of Korea

R. M. Kolonay‡ and M. Blair§

U. S. Air Force Research Laboratory, Wright–Patterson Air Force Base, Ohio 45433

and

R. A. Canfield¶

U. S. Air Force Institute of Technology, Wright–Patterson Air Force Base, Ohio 45433-7765

DOI: 10.2514/1.26869

**The joined wing is a new concept of the airplane wing. The forewing and the aft wing are joined together in a joined wing. The range and loiter are longer than those of a conventional wing. The joined wing can lead to increased aerodynamic performance and reduction of the structural weight. In this research, dynamic response optimization of a joined wing is carried out by using equivalent static loads. Equivalent static loads are made to generate the same displacement field as that from dynamic loads at each time step of dynamic analysis. The gust loads are considered as critical loading conditions and they dynamically act on the structure of the aircraft. It is difficult to identify the exact gust-load profile; therefore, the dynamic loads are assumed to be a one-cosine function. Static response optimization is performed for the two cases: one uses the same design variable definition as dynamic response optimization, and the other uses the thicknesses of all elements as design variables; the results are then compared.**

## I. Introduction

THE joined wing has the advantage of a longer range and loiter than a conventional wing. First, Wolkovich [1] published the joined-wing concept in 1986. Gallman and Kroo [2] offered many recommendations for the design methodology of a joined wing; they used the fully stressed design (FSD) for optimization. Blair et al. [3] initiated nonlinear exploration on a joined-wing configuration in 2005. The U.S. Air Force Research Laboratories (AFRL) have been developing an airplane with the joined wing to complete a long-endurance surveillance mission [4–7]. Figure 1 shows a general joined-wing aircraft. An airplane with a joined wing may be defined as an airplane that has diamond shapes in both top and front views. The forewing and aft wing are joined in the joined wing.

Real loads during flight are dynamic loads. But it is difficult to evaluate exact dynamic loads. Also, dynamic response optimization, which uses dynamic loads directly, is fairly difficult. When the dynamic loads are directly used, there are many time-dependent constraints and the peaks are changed when the design is changed. Because special treatments are required, the technology is rarely applied to large-scale structures [8]. Instead, static response optimization is carried out.

Therefore, static loads, which approximate dynamic loads, were used in structural optimization of the joined wing. However, there are many problems in existing transformation methods. For example, dynamic loads are often transformed to static loads by multiplying

the dynamic factors to the peak of the dynamic loads. But this method does not consider the vibration or inertia properties of the structure. The equivalent static loads are used to overcome these difficulties. The method using equivalent static loads was proposed by Choi and Park [9]. The equivalent static load is defined as a static load that generates the same displacement field as that under a dynamic load. The load is made at each time step of dynamic analysis. The loads are used as multiple loading conditions in structural optimization [8–16].

Size optimization is performed to reduce the structural mass while design conditions are satisfied. Existing static loading conditions are used. Because the condition for the gust load has the most dynamic effect, only the gust loads among the existing static loads are transformed to dynamic loads. Dynamic gust loads are calculated by multiplying static loads by the one-cosine function. Then a coefficient is defined to make the peak of the dynamic load the same as the displacement under the static gust load. The calculated dynamic load is transformed to equivalent static loads for static response optimization. As boundary conditions of the finite element model, the forewing root parts are fixed and the aft-wing root parts are enforced to have certain displacements to maintain stability during flight. NASTRAN and GENESIS are used for size optimization [17,18]. Results from dynamic response optimization using equivalent static loads and static response optimization are compared.

## II. Structural Optimization Under Equivalent Static Loads

Dynamic loads that change in the time domain act on the structures. Static loads are ideal forces that are constant regardless of time. Structures under dynamic loads vibrate and this behavior cannot be represented by the static loads. In many cases, static loads are used for convenience. There are various methods to transform the dynamic loads into static loads. One method of transformation is the equivalent static load method. In structural optimization, the equivalent static loads include the dynamic effects very well.

### A. Transformation of Dynamic Loads into Equivalent Static Loads

An equivalent static load is defined as a static load that makes the same displacement field as that under a dynamic load at an arbitrary time of dynamic analysis. According to the general vibration theory associated with the finite element method (FEM), the structural

Presented at the 11th AIAA/ISSMO Multidisciplinary Analysis and Optimization Conference, Portsmouth, VA, 6–8 September 2006; received 31 July 2006; revision received 21 February 2007; accepted for publication 9 March 2007. Copyright © 2007 by the American Institute of Aeronautics and Astronautics, Inc. All rights reserved. Copies of this paper may be made for personal or internal use, on condition that the copier pay the \$10.00 per-copy fee to the Copyright Clearance Center, Inc., 222 Rosewood Drive, Danvers, MA 01923; include the code 0021-8669/07 \$10.00 in correspondence with the CCC.

\*Graduate Student, Department of Mechanical Engineering.

†Professor, Department of Mechanical Engineering; gjpark@hanyang.ac.kr. Senior Member AIAA (Corresponding Author).

‡Aerospace Engineer, Air Vehicles Directorate. Member AIAA.

§Aerospace Engineer, Air Vehicles Directorate. Associate Fellow AIAA.

¶Associate Professor, Department of Aeronautics and Astronautics. Associate Fellow AIAA.

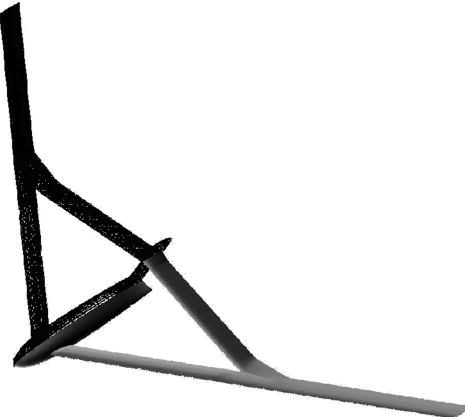


Fig. 1 Joined-wing configuration.

dynamic behavior is presented by the following differential equation:

$$\mathbf{M}(\mathbf{b})\ddot{\mathbf{d}}(t) + \mathbf{K}(\mathbf{b})\mathbf{d}(t) = \mathbf{f}(t) = \{0 \cdots 0 f_i \cdots f_{i+l-1} 0 \cdots 0\}^T \quad (1)$$

where  $\mathbf{M}$  is the mass matrix;  $\mathbf{K}$  is the stiffness matrix;  $\mathbf{f}$  is the vector of external dynamic loads;  $\mathbf{d}$  is the vector of dynamic displacements; and  $l$  is the number of nonzero components of the dynamic load vector. The static analysis with the FEM formulation is expressed as

$$\mathbf{K}(\mathbf{b})\mathbf{x} = \mathbf{s} \quad (2)$$

where  $\mathbf{x}$  is the vector of static displacements and  $\mathbf{s}$  is the vector of external static loads. Equations (1) and (2) are modified to calculate the static load vector that generates an identical displacement field with that from a dynamic load vector at an arbitrary time  $t_a$  as follows:

$$\mathbf{s} = \mathbf{K}\mathbf{d}(t_a) \quad (3)$$

The vector of dynamic displacement  $\mathbf{d}(t_a)$  at a certain time can be obtained from Eq. (1). Substituting  $\mathbf{d}(t_a)$  into Eq. (2), the equivalent static loads are represented as Eq. (3). The static load vector  $\mathbf{s}$ , which is generated by Eq. (3), is an equivalent static load vector that makes the same displacement as that from the dynamic load at a certain time. The global stiffness matrix  $\mathbf{K}$  in Eqs. (2) and (3) can be obtained from the finite element model. Therefore, the equivalent static loads are calculated by multiplication of the global stiffness matrix and the vector of dynamic displacements. The calculated sets of equivalent static loads are used as multiple loading conditions in the optimization process.

### B. Optimization Algorithm with Equivalent Static Loads

The optimization process with equivalent static loads consists of two parts, as illustrated in Fig. 2. They are the analysis domain and the design domain. Based on the results of the analysis domain, equivalent static loads are calculated for the design domain. In the design domain, static response optimization is conducted with the equivalent static loads. The modified design is incorporated to the

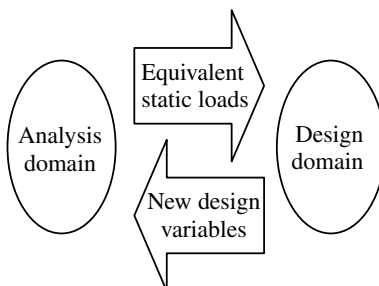


Fig. 2 Schematic process between the analysis domain and the design domain.

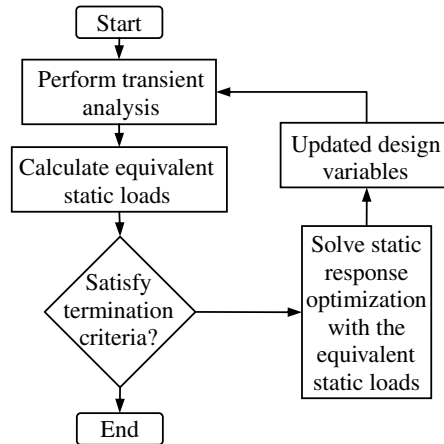


Fig. 3 Optimization process using the equivalent static loads.

analysis domain. The entire optimization process iterates between the two domains until the convergence criteria are satisfied. The circulative procedure between the two domains is defined as the design cycle. The design cycle is performed iteratively. Figure 3 shows the optimization process using equivalent static loads, and the steps of the algorithm are as follows:

Step 1) Set  $p = 0$ ,  $\mathbf{b}_p = \mathbf{b}_0$ .

Step 2) Perform transient analysis in Eq. (1) with  $\mathbf{b}_p$  for  $\mathbf{b}$  (in the analysis domain).

Step 3) Calculate the equivalent static load sets at all time steps by using Eq. (3).

Step 4) When  $p = 0$ , go to step 5.

When  $p > 0$ , if

$$\sum_{i=1}^q \|\mathbf{f}_{\text{eq}}^i(p) - \mathbf{f}_{\text{eq}}^i(p-1)\| < \varepsilon$$

[where  $\mathbf{f}_{\text{eq}}^i(p)$  is the equivalent static load vector at the  $i$ th time step and  $p$ th iteration, and  $\varepsilon$  is a very small value], then terminate. Otherwise, go to step 5.

Step 5. Solve the following static structural optimization problem using various equivalent static loads (in the design domain). Find  $\mathbf{b}$  to minimize  $F(\mathbf{b})$ , subject to

$$\begin{aligned} \mathbf{K}(\mathbf{b})\mathbf{x}_i &= \mathbf{f}_{\text{eq}}^i \quad (i = 1, \dots, \text{no. of time steps}) \\ \Phi(\mathbf{b}, \mathbf{x})_j &\leq 0 \quad (j = 1, \dots, \text{no. of constraints}) \end{aligned} \quad (4)$$

where  $\mathbf{f}_{\text{eq}}$  is the equivalent static load vector used as multiple loading conditions for structural optimization.

Step 6. Set  $p = p + 1$ , and go to step 2.

## III. Analysis of the Joined Wing

### A. Transformation of Dynamic Loads into Equivalent Static Loads

Figure 4 shows a finite element model of the joined wing. The length from the wingtip to the wing root is 38 m and the length of the chord is 2.5 m. The model is composed of 3027 elements that have 2857 quadrilateral elements, 156 triangular elements, and 14 rigid elements. Rigid elements make connections between the nodes of the aft-wing root with the center node of the aft-wing root. The structure has two kinds of aluminum materials: one has Young's modulus of 72.4 GPa, the shear modulus of 27.6 GPa, and the density 2770 kg/m<sup>3</sup>; the other has 36.2 GPa, 13.8 GPa, and 2770 kg/m<sup>3</sup>, respectively [3].

### B. Loading Conditions of the Joined-Wing

Loading conditions for structural optimization are explained; they have been defined by the AFRL [3]. Loading conditions are briefly shown in Table 1, in which  $g$  denotes gravity. There are 11 loading

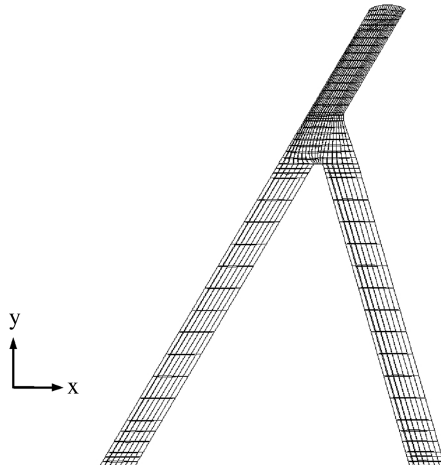


Fig. 4 Finite element modeling of the joined wing.

conditions, which are composed of 7 maneuver loads, 2 gust loads, 1 takeoff load, and 1 landing load.

Gust is the movement of the air in turbulence and the gust load has a large impact on the airplane. Therefore, the gust load is the most important loading condition when an airplane wing is designed [19–22]. The gust load acts dynamically on the airplane. Also, dynamic loads are required for optimization with equivalent static loads. Therefore, the static gust loads of [3] are transformed to dynamic loads because generating exact dynamic loads is difficult. If there is an exact dynamic gust load, it can be directly used without the transformation process introduced here.

Generally, there are several methods for generating dynamic gust loads [23–26]. Here, the approximated dynamic load is evaluated by multiplying the static load by the  $\alpha$  one-cosine function. The coefficient  $\alpha$  is a constant. It is multiplied to a dynamic load to make the dynamic load generate the same displacements at the wingtip as those by static gust loads. The process to obtain the dynamic gust load is explained in the next paragraph.

The duration time of the dynamic gust load is calculated from the following equation [19]:

$$U = \frac{U_{de}}{2} \left( 1 - \cos \frac{2\pi s}{25C} \right) \quad (5)$$

where  $U$  is the velocity of the gust load,  $U_{de}$  is the maximum velocity of the gust load,  $s$  is the distance penetrated into the gust, and  $C$  is the geometric mean chord of the wing. The conditions for the coefficients are shown in Table 2. From Table 2 and Eq. (5), the duration time is 0.374 s.

The dynamic gust load is calculated from Eq. (6):

$$F_{dynamic} = \alpha \times \left( 1 - \cos \frac{2\pi}{0.374} t \right) \times F_{static} \quad (6)$$

Table 1 Load data of the joined wing

Load no.	Load type	Mission leg
1	2.5 g pull up	Ingress
2	2.5 g pull up	Ingress
3	2.5 g pull up	Loiter
4	2.5 g pull up	Loiter
5	2.5 g pull up	Egress
6	2.5 g pull up	Egress
7	2.5 g pull up	Egress
8	Gust (maneuver)	Descent
9	Gust (cruise)	Descent
10	Taxi (1.75 g impact)	Takeoff
11	Impact (3.0 g landing)	Landing

Table 2 Aerodynamic data for the joined wing

Gust maximum velocity	18.2 m/s
Flight velocity	167 m/s
Geometric mean chord of wing	2.5 m
Distance penetrated into gust	62.5 m

where  $F_{static}$  is the static gust load, which is the eighth or ninth load in Table 1. It is noted that the period of the gust load is 0.374 s and the duration time of the dynamic load is 0.374 s.

The process to obtain  $\alpha$  is explained. When loads are imposed on the joined wing, the maximum displacement occurs at the tip. First, the tip displacement is evaluated by the first gust load (the eighth load in Table 1). A dynamic analysis is performed by the dynamic load in Eq. (6) with  $\alpha = 1$ . The maximum displacement of the dynamic analysis is compared with the static tip displacement:  $\alpha$  is the ratio of the two displacements because the two analyses are linear problems, and  $\alpha$  is also evaluated for the second gust load (the ninth load of Table 1); therefore, two dynamic load sets are made.

The following process is carried out for each dynamic gust load. Transient analysis is performed and equivalent static loads are generated. Results of the transient analysis are illustrated in Fig. 5. The tip of the wing vibrates. As illustrated in Fig. 5, the maximum displacement of the wingtip occurs after 0.374 s, which is the duration time of the dynamic load. Also, the maximum displacement occurs within 3 s. The duration time is set by 3 s and the duration is divided into 100 time steps. Therefore, 200 sets of equivalent static loads are generated from the two dynamic gust load cases. There are nine other types of static loads in Table 1, including maneuver loads, taxiing loads, and landing loads. Therefore, the number of the total load cases is 209, which consists of 9 static loads and 200 equivalent static loads; 209 static loading conditions are used as multiple loading conditions in the optimization process.

### C. Boundary Conditions of the Joined-Wing

As illustrated in Fig. 4, the forewing and the aft wing are joined together in the joined wing. Because the root of the forewing is attached to the fuselage, all the degrees of freedom of the six directions are fixed. The six directions are  $x$ -,  $y$ -, and  $z$ -axis translational directions and  $x$ -,  $y$ -, and  $z$ -axis rotational directions, as presented in Fig. 6. The aft wing is also attached to the fuselage at the boundary nodes and the center node, as illustrated in Fig. 6. The center node has an enforced rotation with respect to the  $y$  axis. Each load in Table 1 has a different amount of enforced rotation. The enforced rotation generates torsion on the aft wing and has quite an important aerodynamic effect. The amounts of the enforced rotation are from  $-0.0897$  to  $0$  rad [3]. The boundary nodes are set free in the  $x$  and  $z$  translational directions; other degrees of freedom are fixed. The boundary conditions are illustrated in Fig. 6.

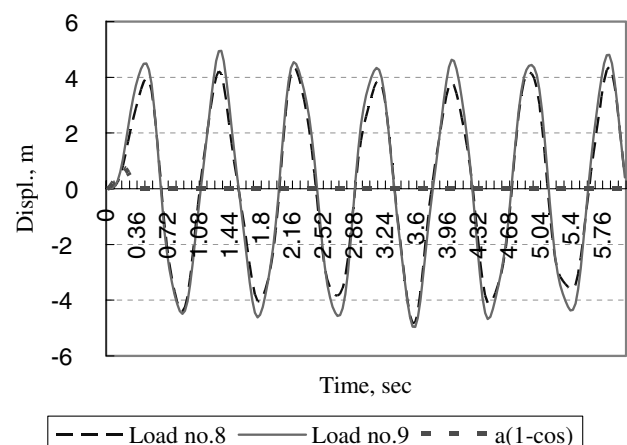


Fig. 5 Vibration of the wingtip deflection.

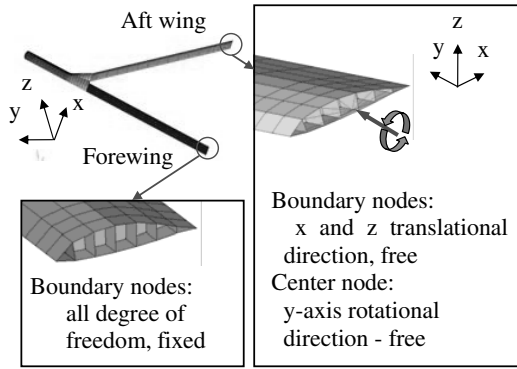


Fig. 6 Boundary conditions of the joined wing.

#### IV. Structural Optimization of the Joined Wing

##### A. Definition of Design Variables

As mentioned earlier, the FEM model has 3027 elements. It is not reasonable to select the properties of all the elements as design variables for optimization. Thus, the design-variable-linking technology is used. The wing structure is divided into 48 sections and each section has the same thickness. The finite element model is adopted from [3]. The model in [3] has a different thickness for 3027 elements. Therefore, each thickness of the 48 sections is made by the average of the element thicknesses in a section. The average value of each section is used as the initial design in the optimization process.

First, the joined wing is divided into five parts, which are the forewing, the aft wing, the midwing, the wingtip, and the edge around the joined wing. The parts are illustrated in Fig. 7. Each part is composed of the top skin, the bottom skin, the spar, and the rib. The top and bottom skins are divided into three sections. Only 43 sections among the 48 sections are used as design variables. Figure 8 presents the division for the midwing; the forewing, the aft wing, the wingtip, and the edge are divided in the same manner. The spar of the tip wing and the top skin, the bottom skin, and the rib of the edge part are not used as design variables. Design variables are defined based on the [3].

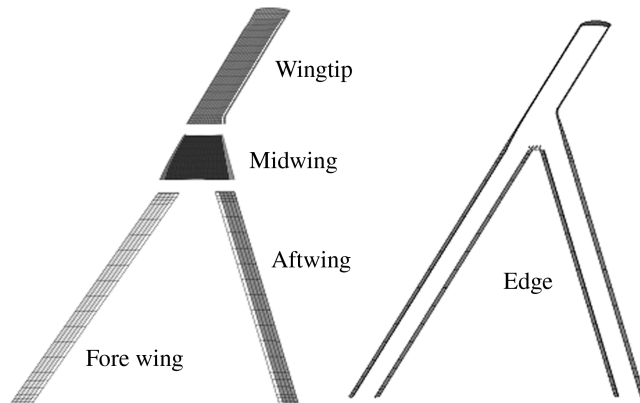


Fig. 7 Five parts for definition of design variables.

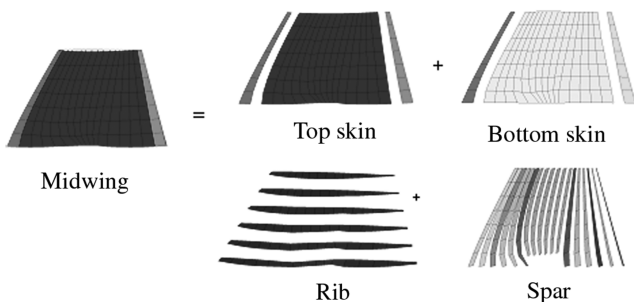


Fig. 8 Sections for definition of design variables.

Table 3 Results of the objective function of case 1

Iteration no.	Optimum value, kg	Constraint violation, %
0	4199.7	142.1 (216.009)
1	4855.8	68.4
2	4778.9	105.5
...	...	...
23	4755.2	0.5
24	4755.1	1.3 (190.307)

##### B. Formulation

The formulation for optimization is

Find  $t_i$  ( $i = 1, \dots, 43$ ) to minimize mass, subject to

$$\begin{aligned} |\sigma_j| &\leq \sigma_{\text{allowable}} \quad (j = 1, \dots, 2559) \\ 0.001016 \text{ m} &\leq t_i \leq 0.3 \text{ m} \quad (i = 1, \dots, 43) \end{aligned} \quad (7)$$

The initial model in [3] has 3027 elements and each element has a different thickness. The mass of the initial model is 4199.7 kg. Static response optimization is carried out for the initial model. As mentioned earlier, the initial model is divided into 48 sections, and the initial thickness is defined by the average value. The mass of this modified model is 4468.6 kg. This model is used in static response optimization and dynamic response optimization using equivalent static loads.

The material of the joined wing is aluminum. The allowable von Mises stress for aluminum is set by 253 MPa. Because the safety factor 1.5 is used, the allowable stress is reduced to 169 MPa [3]. Stresses of all the elements except for the edge part should be less than the allowable stress of 169 MPa. Lower and upper bounds of the design variables are set by 0.001016 and 0.3 m, respectively.

#### V. Results of Discussion

##### A. Optimization Results

The results from dynamic response optimization with equivalent static loads are compared with the results from static response optimization. Static response optimization is performed for two cases with different definitions of design variables. Case 1 and case 2 are static response optimizations and case 3 is dynamic response optimization.

Case 1 is the static response optimization with the 11 loads in Table 1. In the model of case 1, the thickness of all elements is different and the starting mass is 4199.7 kg. Design variables are thicknesses of the structure, except for the edge part of the joined wing. The number of design variables is 2559. Constraints are imposed on the stresses as Eq. (7). Table 3 and Fig. 9 show the results of optimization. Constraint violation in Table 3 is the value when static response optimization is performed; the value in parenthesis is the value when transient analysis is performed with the design. As shown in Table 3, the constraints are satisfied in the static response

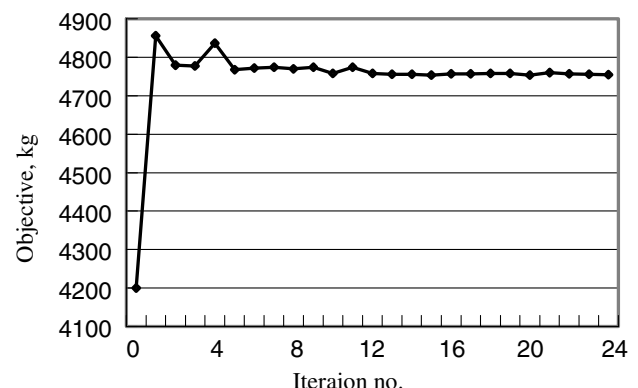


Fig. 9 The history of the objective function of case 1.

**Table 4** Results of the objective function of case 2

Iteration no.	Optimum value, kg	Constraint violation, %
0	4468.60	173.83 (344.21)
1	9391.202	25.055
2	10,759.24	0.600
3	10,901.66	0.204
4	10,901.66	0.204 (49.561)

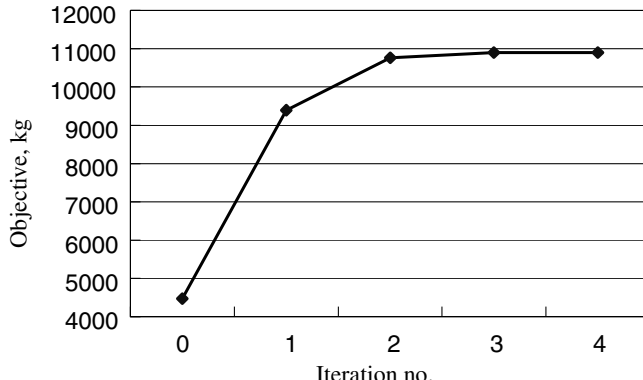
optimization process. But when transient analysis is performed with the optimum solution, it is noted that the constraints are violated; that is, static response optimization is not sufficient for a dynamic system. The static response optimization process converges in 24 iterations, and the CPU is 29 h and 30 min with an HP Unix Itanium 1.6 GHz CPU 4. The objective function increases about 13.2% from 4199.7 to 4755.1 kg. The commercial software GENESIS is used for the optimization process [17] and transient analysis is performed by NASTRAN [18].

Case 2 is performed under the same loading condition as case 1. The model for case 2 has 48 sections. The starting value of the mass is 4468.6 kg. The loading conditions are the same as those of case 1. The formulation of the optimization process is shown in Eq. (7). As mentioned earlier, there are 43 design variables. The history of the optimization process is shown in Table 4 and Fig. 10. Constraint violation in Table 4 is expressed in the same way as in Table 3. In case 2, the constraints are satisfied in the optimization process. When transient analysis is performed with the optimum solution, the stress constraints are violated. The process converges in four iterations and the CPU time is 30 min. The mass increases about 144% from 4468.6 to 10,901.66 kg. The commercial software for the optimization process is NASTRAN [18] and the computer is an AMD Athlon 64-bit processor with 2.01 GHz and 1.0 GB RAM.

Case 3 uses dynamic response optimization. The dynamic loads are those explained in Sec. III.B. The design variables are the same as those of case 2. Dynamic loads are made for the two gust loads in Table 1 and equivalent static loads are generated. As explained in Sec. III.B, 209 loading conditions are used in a static response optimization process. The model of case 3 is equal to the model of case 2. The process converges in 10 cycles. One cycle is a process between the analysis domain and the design domain. The total CPU time is 21 h and 10 min. As shown in Table 5, the mass of the joined wing is increased by 184.8% from the initial mass. It is noted that the constraints are satisfied when transient analysis is performed with the optimum solution. Then commercial software system and the computer used for the optimization process are the same as those of case 2.

## B. Discussion

Figure 12a shows the results of design variables from case 1. Part A in Fig. 12c has the lower bound, and the optimum values of part B are larger than 1 cm. Generally, the wingtip has the lower

**Fig. 10** The history of the objective function of case 2.**Table 5** Results of the objective function of case 3

Iteration no.	Optimum value, kg	Constraint violation, %
0	4468.60	344.213
1	16,527.18	-16.427
2	9329.58	40.759
3	14,172.92	66.899
4	10,610.69	23.755
5	13,579.97	18.86
6	10,852.17	14.993
7	11,782.34	6.196
8	12,112.68	8.368
9	12,918.26	1.26
10	12,725.52	0.681

bound and the thickness of the aft wing is larger than that of the forewing.

The results of the top and bottom skins of the aft wing are illustrated in Fig. 12b for case 2 and case 3. The thicknesses of the skins of the aft wing become larger compared with the initial thicknesses. The parts A and B of the top skin in Fig. 12b have thicknesses three times larger than that of case 2; part C has four times larger thickness.

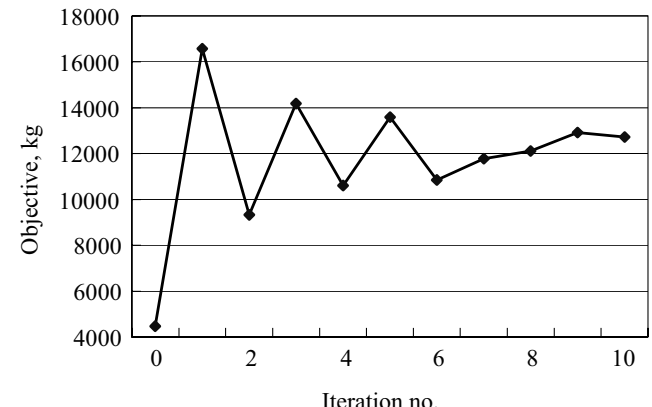
The changes of the spar of the aft wing are shown in Fig. 12c. In part A of Fig. 12c, the optimum thickness of case 2 is 2.3 times larger than that of case 3. The results of the two cases are similar for part B in Fig. 12c. The thickness of part C becomes larger than the initial thickness in case 2, but it is reduced by 70% in case 3. Figure 12d shows the results at the spar of the midwing. It is noted that the results of static response optimization and dynamic response optimization are considerably different.

Transient analysis with optimum solutions is performed for the three cases to verify the optimization results. Stress distribution of each case is shown in Fig. 13 when the maximum stress occurs. As shown in Fig. 13a, the maximum stress of case 1 occurs at the top skin of the forewing. The magnitude of the stress is 490 MPa and it occurs at the time of 1.17 s. The stress contour for case 2 is illustrated in Fig. 13b. The maximum stress is 253 MPa at the top skin of the aft-wing root at the time of 2.55 s. Figure 13c is for case 3. The maximum stress occurs at the time of 1.26 s and it is 170 MPa at the top skin of the midwing.

The maximum stresses of the three cases have different magnitudes and locations. When transient analysis is performed, constraints are violated in case 1 and case 2, whereas they are satisfied in case 3. Therefore, optimization with equivalent static loads accommodates the dynamic characteristics quite well.

## VI. Conclusions

A joined wing, which has a longer range and loiter than a conventional wing, is investigated from the viewpoint of weight reduction. Structural optimization considering dynamic effect is

**Fig. 11** The history of the objective function of case 3.

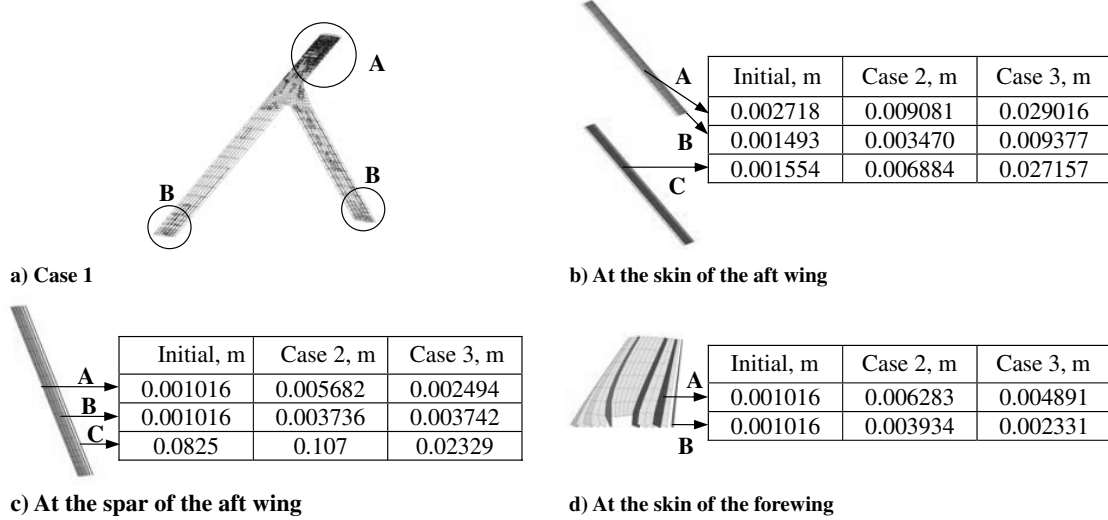


Fig. 12 Results of the design variables.

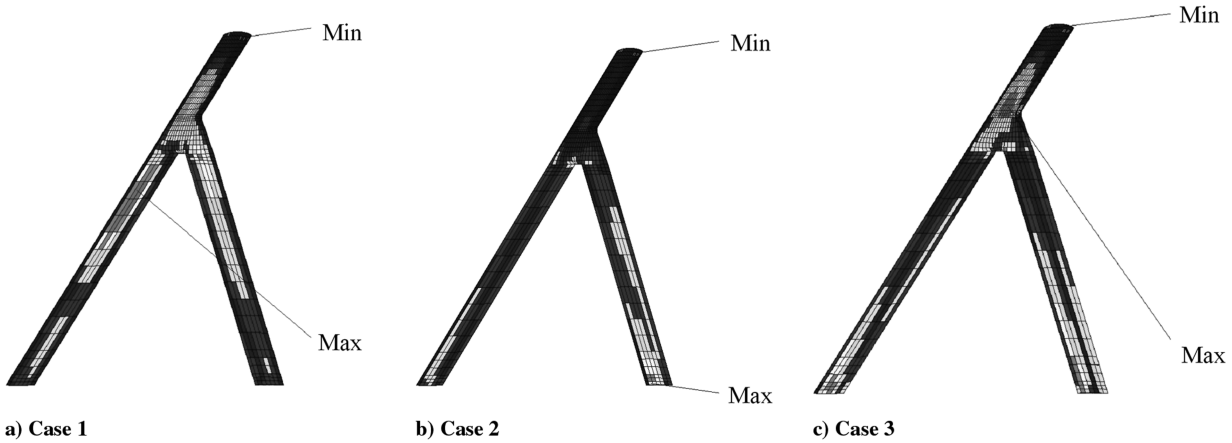


Fig. 13 Stress contour.

required due to the characteristics of the aircraft, which must endure dynamic loads. Especially, gust loads should be considered in the design of the aircraft. Calculating exact dynamic gust load is difficult in that complicated aeroelastic analysis is required. Therefore, approximated dynamic gust loads are evaluated using an approximation method. The function (one cosine) is used for the approximation. Structural optimization is performed for mass reduction by using equivalent static loads. An equivalent static load is a static load that makes the same displacement field as that under a dynamic load at an arbitrary time. The equivalent static load can consider the exact dynamic effect compared with the conventional dynamic factors.

When transient analysis is performed, it is found that the maximum stress of the initial design is three times the allowable stress. Static response optimization is carried out based on the given loads. When transient analysis is performed with the optimum solution of static response optimization, the constraint is violated by 50%. However, the optimization results with equivalent static loads satisfy the constraints. It is found that the equivalent static loads accommodate the dynamic effect very well.

The dynamic load for the equivalent static loads is calculated by using the approximation method of the one-cosine function. In the future, it will be necessary to generate exact dynamic loads by using aeroelastic analysis. Also, the deformation of the joined wing is considerably large in the elastic range; it has geometric nonlinearity. The fully stressed design algorithm was used with nonlinear static analysis of the joined wing [3]. It will be necessary to perform structural optimization considering the nonlinearity of the joined wing using equivalent static loads.

## Acknowledgments

This work was supported by the U.S. Air Force (AOARD-05-4015) and the Center of Innovative Design Optimization Technology, which was founded by the Korea Science and Engineering Foundation. The authors are thankful to MiSun Park for her correction of the manuscript.

## References

- [1] Volkovich, J., "The Joined-Wing: An Overview," *Journal of Aircraft*, Vol. 23, No. 3, 1986, pp. 161–178.
- [2] Gallman, J. W., and Kroo, I. M., "Structural Optimization of Joined-Wing Synthesis," *Journal of Aircraft*, Vol. 33, No. 1, 1996, pp. 214–223.
- [3] Blair, M., Canfield, R. A., and Roberts, R. W., "Joined-Wing Aeroelastic Design with Geometric Nonlinearity," *Journal of Aircraft*, Vol. 42, No. 4, 2005, pp. 832–848.
- [4] Blair, M., and Canfield, R. A., "A Joined-Wing Structural Weight Modeling Study," *AIAA/ASME/ASCE/AHS/ASC Structures, Structural Dynamics, and Materials Conference*, Vol. 2, AIAA, Reston, VA, 2002, pp. 1068–1078.
- [5] Roberts, R. W., Canfield, R. A., and Blair, M., "Sensor-Craft Structural Optimization and Analytical Certification," *AIAA/ASME/ASCE/AHS/ASC Structures, Structural Dynamics, and Materials Conference*, Vol. 1, AIAA, Reston, VA, 2003, pp. 539–548.
- [6] Rasmussen, C. C., Canfield, R. A., and Blair, M., "Joined-Wing Sensor-Craft Configuration Design," *Journal of Aircraft*, Vol. 43, No. 5, 2006, pp. 1470–1478.
- [7] Rasmussen, C. C., Canfield, R. A., and Blair, M., "Optimization Process for Configuration of Flexible Joined-Wing," *10th AIAA/ISSMO Multidisciplinary Analysis and Optimization Conference*, AIAA,

Reston, VA, 2004, pp. 1–9.

[8] Kang, B. S., Park, G. J., and Arora, J. S., “A Review of Optimization of Structures Subjected to Transient Loads,” *Structural and Multidisciplinary Optimization*, Vol. 31, Feb. 2006, pp. 81–95.

[9] Choi, W. S., and Park, G. J., “Transformation of Dynamic Loads into Equivalent Static Loads Based on Model Analysis,” *International Journal for Numerical Methods in Engineering*, Vol. 46, No. 1, 1999, pp. 29–43.

[10] Choi, W. S., and Park, G. J., “Quasi-Static Structural Optimization Technique Using Equivalent Static Loads Calculated at Every Time Step as a Multiple Loading Condition,” *Transactions of the Korean Society of Mechanical Engineers (A)*, Vol. 24, No. 10, 2000, pp. 2568–2580.

[11] Choi, W. S., and Park, G. J., “Structural Optimization Using Equivalent Static Loads at All the Time Intervals,” *Computer Methods in Applied Mechanics and Engineering*, Vol. 191, No. 19, 2002, pp. 2077–2094.

[12] Kang, B. S., Choi, W. S., and Park, G. J., “Structural Optimization Under Equivalent Static Loads Transformed from Dynamic Loads Based on Displacement,” *Computers and Structures*, Vol. 79, No. 2, 2001, pp. 145–154.

[13] Park, G. J., and Kang, B. S., “Mathematical Proof for Structural Optimization with Equivalent Static Loads Transformed from Dynamic Loads,” *Transactions of the Korean Society of Mechanical Engineers (A)*, Vol. 27, No. 2, 2003, pp. 268–275.

[14] Park, G. J., and Kang, B. S., “Validation of a Structural Optimization Algorithm Transforming Dynamic Loads into Equivalent Static Loads,” *Journal of Optimization Theory and Applications*, Vol. 118, No. 1, 2003, pp. 191–200.

[15] Park, K. J., Lee, J. N., and Park, G. J., “Structural Shape Optimization Using Equivalent Static Loads Transformed from Dynamic Loads,” *International Journal for Numerical Methods in Engineering*, Vol. 63, No. 4, 2005, pp. 589–602.

[16] Kang, B. S., Park, G. J., and Arora, J. S., “Optimization of Flexible Multibody Dynamic Systems Using the Equivalent Static Loads,” *AIAA Journal*, Vol. 43, No. 4, 2005, pp. 846–852.

[17] GENESIS User’s Manual, Ver. 7.0, Vanderplaats Research and Development, Inc., Colorado Springs, CO, 2001.

[18] MSC.NASTRAN 2004 Reference Manual, Ver. 2004, MSC. Software Corp., Santa Ana, CA, 2003.

[19] Hoblit, F. M., *Gust Loads on Aircraft: Concepts and Applications*, AIAA, Washington, D.C., 1988, Chaps. 2, 3.

[20] Megson, T. H. G., *Aircraft Structures*, 3rd ed., Butterworth Heinemann, London, 1999, Chap. 8.

[21] Kareem, A., and Zhou, Y., “Gust Loading Factor-Past, Present and Future,” *Journal of Wind Engineering and Industrial Aerodynamics*, Vol. 91, Nos. 12/15, 2003, pp. 1301–1328.

[22] Corke, T. C., *Design of Aircraft*, Prentice–Hall, Upper Saddle River, NJ, 2002, Chaps. 7, 8, 10.

[23] Rao, S. S., “Optimization of Airplane Wing Structures Under Gust Loads,” *Computers and Structures*, Vol. 21, No. 4, 1985, pp. 741–749.

[24] Noback, R., “Comparison of Discrete and Continuous Gust Methods for Airplane Design Loads Determination,” *Journal of Aircraft*, Vol. 23, No. 3, 1986, pp. 226–231.

[25] Fuller, J. R., “Evolution of Airplane Gust Loads Design Requirements,” *Journal of Aircraft*, Vol. 32, No. 2, 1995, pp. 235–246.

[26] Singh, R., and Baeder, J. D., “Generalized Moving Gust Response Using CFD with Application to Airfoil-Vortex Interaction,” *AIAA Applied Aerodynamics Conference*, AIAA, Reston, VA, 1997, pp. 25–35.